

Physical Conditions and Particle Acceleration in the Kiloparsec Jet of Centaurus A

TAKAHIRO SUDOH,¹ DMITRY KHANGULYAN,² AND YOSHIYUKI INOUE^{3,4}

¹*Department of Astronomy, University of Tokyo, Hongo, Tokyo 113-0033, Japan*

²*Department of Physics, Rikkyo University, Nishi-Ikebukuro 3-34-1, Toshima-ku, Tokyo 171-8501, Japan*

³*Interdisciplinary Theoretical & Mathematical Science Program (iTHEMS), RIKEN, 2-1 Hirosawa, Saitama 351-0198, Japan*

⁴*Kavli Institute for the Physics and Mathematics of the Universe (WPI), UTIAS, The University of Tokyo, Kashiwa, Chiba 277-8583, Japan*

ABSTRACT

The non-thermal emission from the kiloparsec-scale jet of Centaurus A exhibits two notable features, bright diffuse emission and many compact knots, which have been intensively studied in X-ray and radio observations. H.E.S.S. recently reported that the very-high-energy gamma-ray emission from this object is extended along the jet direction beyond a kiloparsec from the core. Here, we combine these observations to constrain the physical conditions of the kpc-jet and study the origin of the non-thermal emission. We show that the diffuse jet is weakly magnetized ($\eta_B \sim 10^{-2}$) and energetically dominated by thermal particles. We also show that knots are the sites of both amplified magnetic field and particle (re-)acceleration. To keep sufficient energy in thermal particles, the magnetic and non-thermal particle energy in the knot regions are tightly constrained. The most plausible condition is an energy equipartition between them, $\eta_B \sim \eta_e \sim 0.1$. Such weak magnetic energy implies that particles in the knots are in the slow cooling regime. We suggest that the entire kpc-scale diffuse emission could be powered by particles that are accelerated at and escaped from knots.

1. INTRODUCTION

It is widely believed that jets from active galactic nuclei (AGN) are launched by electromagnetic mechanisms near supermassive black holes (SMBH) (e.g., Blandford & Znajek 1977; Blandford & Payne 1982; Komissarov et al. 2007; McKinney et al. 2012). As a result, jets are expected to be initially highly magnetized. The dissipation of the magnetic field converts the Poynting flux into the bulk kinetic energy, accelerating the jet to a relativistic speed. A fraction of the jet power is also transferred to particles, heating the jet material and accelerating particles to non-thermal energies. Particle acceleration can proceed effectively either in a magnetically-dominated (e.g., via magnetic reconnection) or kinetically-dominated (e.g., via formation of shocks) jet (e.g., Sironi et al. 2015). Therefore, to understand the production mechanism of non-thermal particles, the determination of the energy balance in the jets, especially their magnetization, is essential.

Observational studies of energy balance in AGN jets are mostly conducted for blazars, i.e., radio galaxies with

their jets aligned toward Earth (e.g., Tavecchio et al. 1998; Celotti & Ghisellini 2008; Ghisellini et al. 2010; Zhang et al. 2012; Inoue & Tanaka 2016). These studies typically find relatively weak magnetization. However, they are usually restricted to one-zone treatment aimed to explain observations at various phases. As blazars are highly variable (e.g., Ackermann et al. 2016), it is unclear whether the emission of each phase correctly probes the conditions in the large-scale jet. Most blazars are located at cosmological distances, which makes any study beyond one-zone treatment difficult.

The radio galaxy Centaurus A (Cen A) enables invaluable insights on this problem thanks to its unequalled proximity (3.8 Mpc; Harris et al. 2010). Broadband emission from this object has been resolved over a wide range of spatial scales from the core ($\lesssim 10^{-2}$ pc) to the giant lobes ($\gtrsim 10^5$ pc) (e.g., Kraft et al. 2002; Hardcastle et al. 2006; Kataoka et al. 2006; Goodger et al. 2010). Recently, the H.E.S.S. collaboration has reported evidence of very-high-energy (VHE) gamma rays from the kpc-scale jet in Cen A (Abdalla et al. 2020), making it the first extragalactic object with measured extension in the VHE regime. A combination of new gamma-ray data with previous multi-wavelength data brings new information on jet properties on kpc distances from SMBH.

Here, we study the origin of non-thermal emission and physical conditions of the kpc-jet in Cen A. Our approach is model-independent, meaning that we rely on observational data only. In Sec. 2, we summarize observational properties. In Sec. 3, we constrain the physical conditions in the jet required from X-ray observations. In Sec. 4, we further constrain the parameter space with the VHE data. In Sec. 5, we discuss contributions from hadronic emission. In Sec. 6, we summarize our findings.

2. OBSERVATIONAL PROPERTIES

The SMBH at the core of Cen A has a mass of $5.5 \times 10^7 M_\odot$ measured by stellar kinematics (Cappellari et al. 2009), with corresponding Eddington luminosity of $7 \times 10^{45} \text{ erg s}^{-1}$. It provides an ultimate energy source to the jet, which has an estimated power of $\sim 10^{43} \text{ erg s}^{-1}$ (Wykes et al. 2013), a bulk velocity of $\simeq 0.5c$ (Hardcastle et al. 2003a) on a hundred-parsec scale, and an opening angle of $10^\circ - 15^\circ$ (e.g., Horiuchi et al. 2006).

On kpc scales, the jet produces diffuse synchrotron emission. Kataoka et al. (2006) utilized *Chandra* data and obtained the X-ray flux along the jet from the core up to about $240''$ (4 kpc). The observed 0.5–5 keV luminosity of the diffuse unresolved kpc-scale jet is $L_{\text{keV}}^{\text{D}} \simeq 8 \times 10^{38} \text{ erg s}^{-1}$, where the superscript D stands for the diffuse component. We define this energy range as the keV band. The spectral index of this component, $\alpha = -d \ln F_\nu / d \ln \nu$, is consistent with $\alpha \simeq 1$.

The jet contains individual knots resolved in X-ray and radio observations (Kraft et al. 2002; Goodger et al. 2010). The number of X-ray knots identified in Kataoka et al. (2006) is about 30. While $\sim 2 - 5$ of them could be low-mass X-ray binaries unrelated to the jet emission (Goodger et al. 2010), the majority are produced by the jet material (Blandford & Koenigl 1979; Sanders 1983; Hardcastle et al. 2003b; Mao & Wang 2007; Bednarek & Banasiński 2015; Vieyro et al. 2017; Torres-Albà & Bosch-Ramon 2019). The typical keV-band luminosity of each knot is $L_{\text{keV}}^{\text{K}} \simeq 10^{37} \text{ erg s}^{-1}$, where the superscript K stands for knots. The X-ray spectral indices are consistent with $\alpha \simeq 0.5 - 1$ (Goodger et al. 2010; Tanada et al. 2019). For some knots, the spectral indices in radio band (4.8–8.4 GHz) are also measured, in the range of $\alpha \simeq 0.5 - 2$, although measurement errors are large (Goodger et al. 2010).

The sizes of knots are constrained only for some of the brightest ones, typically $\simeq 2 - 10 \text{ pc}$ (Tingay & Lenc 2009; Goodger et al. 2010; Tanada et al. 2019). The magnetic fields in the knots are also largely unconstrained. For two bright knots, BX2 and AX1C, *Chandra* observations suggest upper limits of $B \lesssim 80 \mu\text{G}$ due

Table 1. Luminosity of the host galaxy NGC 5128

Band	Wavelength [μm]	Luminosity [erg s^{-1}]
optical	0.6	$\sim 9 \times 10^{43}$
near-IR	2	$\sim 6 \times 10^{43}$
mid-IR	25	$\sim 0.6 \times 10^{43}$
far-IR	100	$\sim 2 \times 10^{43}$

to the absence of spectral steepening expected for synchrotron cooling (Snios et al. 2019).

The production of synchrotron emission in the energy of $\epsilon = 1\epsilon_1 \text{ keV}$ implies the presence of electrons with energy of $E_e \simeq 10\epsilon_1^{1/2} B_{100}^{-1/2} \text{ TeV}$, where $B = 100B_{100} \mu\text{G}$ is the magnetic field strength. The same population of electrons produces gamma rays by inverse Compton (IC) scattering. If the scattering proceeds in the Thomson regime, the characteristic gamma-ray energy is

$$\epsilon_{\text{IC}} = 300 \left(\frac{\hbar\omega_0}{6 \times 10^{-4} \text{ eV}} \right) \left(\frac{E_e}{10 \text{ TeV}} \right)^2 \text{ GeV}, \quad (1)$$

where $\hbar\omega_0$ is the energy of target photons, and the Thomson limit is valid for $\hbar\omega_0 \ll 0.1 (E_e/10 \text{ TeV})^{-1} \text{ eV}$. The recent H.E.S.S. analysis has confirmed that VHE emission is produced in the kpc-jet (Abdalla et al. 2020). The flux is approximately $2 \times 10^{-10} \text{ GeV cm}^{-2} \text{ s}^{-1}$ at $\epsilon_{\text{IC}} \simeq 300 \text{ GeV}$ and the spectrum is fit by a power-law with $\alpha \simeq 1.5$ up to $\sim 10 \text{ TeV}$ (H. E. S. S. Collaboration et al. 2018). Thus, the luminosity in VHE band, which we define as 0.3–3 TeV, is $L_{\text{VHE}} \simeq 7 \times 10^{38} \text{ erg s}^{-1}$.

The target photon fields may be produced by the jet itself and objects in it and also supplied by external sources. The host galaxy provides the brightest external soft photons in optical and infrared. Table 1 shows characteristics of soft photons from the host galaxy taken from NASA/IPAC Extragalactic Database. Note that they may not be taken at face values, because soft photons with a shorter wavelength are affected by Klein–Nishina suppression. For example, for an electron spectrum of $dN_e/dE_e \propto E_e^{-3}$, the contributions from optical and near-IR are smaller than that of far-IR above $\epsilon_{\text{IC}} \simeq 100 \text{ GeV}$, even though they have higher luminosities. The nucleus of Cen A could also provide target photons with a bolometric luminosity of $\sim 10^{43} \text{ erg s}^{-1}$ (Chiaberge et al. 2001; Beckmann et al. 2011).

3. CONSTRAINTS FROM X-RAY DATA

3.1. Jet Energy Balance

The average physical conditions in the jet are determined by its basic properties. We assume that the kpc jet is cylindrical with a radius R and height $Z =$

$3Z_3$ kpc, starting from a distance of 1 kpc from the core. We use an opening angle of $\theta = 0.2\theta_{0.2}$ rad, which results in $R = 200\theta_{0.2}$ pc. This might appear an overestimate for the jet radius at 1 kpc (e.g., Wykes et al. 2019). However, since we adopt a cylindrical approximation, we consider it to be appropriate as the mean radius of the kpc jet. We assume a total jet power of $P_{\text{jet}} = 10^{43} P_{43} \text{ erg s}^{-1}$. The energy flux in the jet is

$$\frac{P_{\text{jet}}}{\pi R^2} \simeq 8 P_{43} \theta_{0.2}^{-2} \text{ erg s}^{-1} \text{ cm}^{-2}. \quad (2)$$

The jet bulk speed, $\beta = 0.5\beta_{0.5}$, defines the energy density

$$w_{\text{jet}} = \frac{P_{\text{jet}}}{\pi R^2 \beta c} \simeq 350 P_{43} \theta_{0.2}^{-2} \beta_{0.5}^{-1} \text{ eV cm}^{-3}, \quad (3)$$

which is distributed to thermal gas (or plasma), magnetic field, and non-thermal protons and electrons, such that

$$w_{\text{Th}} + w_{\text{B}} + w_{e,\text{NT}} + w_{p,\text{NT}} = w_{\text{jet}}. \quad (4)$$

We define the corresponding fractions, $\eta_i = w_i/w_{\text{jet}}$:

$$\eta_{\text{Th}} + \eta_{\text{B}} + \eta_{e,\text{NT}} + \eta_{p,\text{NT}} = 1. \quad (5)$$

The magnetic energy density,

$$w_{\text{B}} = \frac{B^2}{8\pi} = \eta_{\text{B}} w_{\text{jet}}, \quad (6)$$

converts to the strength of the magnetic field:

$$B = \sqrt{\frac{8\pi\eta_{\text{B}}P_j}{\pi R^2\beta c}} = 120 \sqrt{\frac{\eta_{\text{B}}P_{43}}{\beta_{0.5}}} \theta_{0.2}^{-1} \mu\text{G}. \quad (7)$$

The energy distribution for non-thermal particles is often approximated with a broken power law:

$$\frac{dn_Y}{dE dV} = \begin{cases} A_Y (E/E_{Y,\text{br}})^{-p_{Y,H}} & E \geq E_{Y,\text{br}}, \\ A_Y (E/E_{Y,\text{br}})^{-p_{Y,L}} & E_{Y,\text{min}} < E \leq E_{Y,\text{br}}. \end{cases} \quad (8)$$

Here Y denotes the particle type, $p_{Y,L}$ and $p_{Y,H}$ define power-law slopes, $E_{Y,\text{br}}$ is the break energy, A_Y is the normalization, and $E_{Y,\text{min}}$ is the minimum energy of the non-thermal distribution. The energy density in non-thermal particles is

$$w_{Y,\text{NT}} = \int_{E_{Y,\text{min}}}^{\infty} \frac{dn_Y}{dE dV} E dE. \quad (9)$$

For electrons, radio-emitting particles typically have low energy ($E_e < E_{e,\text{br}}$), while X-ray emitting particles have high energy ($E_e > E_{e,\text{br}}$). Therefore, the energy

content in non-thermal electrons that produce emission in the keV-band is

$$w_{e,\text{keV}} = A_e \int_{\sqrt{0.5}E_{e,\text{keV}}}^{\sqrt{5}E_{e,\text{keV}}} \left(\frac{E}{E_{e,\text{br}}} \right)^{-p_{e,H}} E dE, \quad (10)$$

where $E_{e,\text{keV}}$ is the energy of electrons which are responsible for the production of 1 keV synchrotron photons: $E_{e,\text{keV}} \simeq 10 (B/100 \mu\text{G})^{-1/2} \text{ TeV}$. It is useful to define another parameter,

$$\chi_{\text{keV}} = \frac{w_{e,\text{keV}}}{w_{e,\text{NT}}} = \frac{\eta_{e,\text{keV}}}{\eta_{e,\text{NT}}}, \quad (11)$$

which is determined by the electron spectrum.

3.2. X-ray Emission from the Jet

X-ray observations of Cen A revealed both diffuse unresolved emission and many compact knots in the kpc jet. The diffuse jet luminosity in the keV band is $L_{\text{keV}}^{\text{D}} \simeq 8 \times 10^{38} \text{ erg s}^{-1}$ (Kataoka et al. 2006), and the volume is $V^{\text{D}} \simeq \pi R^2 Z \simeq 10^{64} \theta_{0.2}^2 Z_3 \text{ cm}^3$. The luminosity density, $j = L/V$, of the diffuse jet is

$$j_{\text{keV}}^{\text{D}} = 7 \times 10^{-26} \theta_{0.2}^{-2} Z_3^{-1} \text{ erg s}^{-1} \text{ cm}^{-3} \quad (12)$$

The compact knots have a typical keV-band luminosity of $L_{\text{keV}}^{\text{K}} = 10^{37} L_{37} \text{ erg s}^{-1}$. We adopt a characteristic knot size of $r = 5r_5$ pc and assume that knots are spherical. Then, the typical volume is $V^{\text{K}} = 2 \times 10^{58} r_5^3 \text{ cm}^3$. The luminosity density of the knot radiation is

$$j_{\text{keV}}^{\text{K}} = 6 \times 10^{-22} r_5^{-3} L_{37} \text{ erg s}^{-1} \text{ cm}^{-3}. \quad (13)$$

These luminosities are determined by the energy content in keV-emitting electrons and their synchrotron cooling time,

$$t_{\text{syn}} \simeq 2 \times 10^2 \left(\frac{\hbar\omega}{1 \text{ keV}} \right)^{-1/2} \left(\frac{w_{\text{B}}}{100 \text{ eV cm}^{-3}} \right)^{-3/4} \text{ yr}, \quad (14)$$

where $\hbar\omega$ is the synchrotron emission energy. By equating j_{keV} with $w_{e,\text{keV}}/t_{\text{syn}}$, we obtain the following constraints on the production sites of synchrotron emission:

$$(\eta_{\text{B}}^{\text{D}})^{3/4} \eta_{e,\text{keV}}^{\text{D}} \simeq 3 \times 10^{-7} \theta_{0.2}^{3/2} Z_3^{-1} \beta_{0.5}^{7/4} P_{43}^{-7/4} \quad (15)$$

and

$$(\eta_{\text{B}}^{\text{K}})^{3/4} \eta_{e,\text{keV}}^{\text{K}} r_5^3 \simeq 3 \times 10^{-3} L_{37} \theta_{0.2}^{7/2} \beta_{0.5}^{7/4} P_{43}^{-7/4}. \quad (16)$$

To relate $\eta_{e,\text{keV}}$ to $\eta_{e,\text{NT}}$, we need the electron spectrum. In general, the ratio of these two, χ_{keV} , is larger for a harder spectrum. For the diffuse jet, Hardcastle & Croston (2011) derived $p_{e,L} \simeq 2.06$ for radio-emitting

electrons and a very steep spectrum for X-ray emitting particles, $p_{e,H} \simeq 3.88$ and $E_{e,br} \sim 10^{-1.5} E_{e,kev}$, based on multi-wavelength data (Hardcastle et al. 2006). If we assume $E_{e,min} \sim 10^{-3} E_{e,br}$, these values convert to $\chi_{kev}^D \sim 10^{-4}$. We note that this spectrum is obtained from about 2–4 arcmin (2–4 kpc) from the core. Closer to the core, the X-ray spectrum may be harder. Indeed, the X-ray spectrum derived in Kataoka et al. (2006) for the 1–2 kpc jet yields $p_{e,H} \simeq 3.0 - 3.4$, resulting in $\chi_{kev}^D \sim 10^{-3}$. Therefore, the value of χ_{kev}^D averaged over the kpc-jet is likely larger than 10^{-4} . Utilizing this, we rewrite Eq. (15) as

$$(\eta_B^D)^{3/4} \eta_{e,NT}^D \simeq 3 \times 10^{-3} \theta_{0.2}^{3/2} Z_3^{-1} \beta_{0.5}^{7/4} P_{43}^{-7/4} \chi_{-4}^{-1}, \quad (17)$$

where $\chi_{-4} = \chi_{kev}^D / 10^{-4}$. We constrain the jet parameters by requiring that the sum of non-thermal electron and magnetic energy, $\eta_B^D + \eta_{e,NT}^D$, is less than one. Figure 1 shows this sum under the above constraint (Eq. 17) as a function of η_B^D . This shows that a wide range of η_B^D and $\eta_{e,NT}^D$ is allowed from the X-ray data.

The spectral properties of knots are less tightly constrained from observations and may differ from one to another. However, observed X-ray fluxes can place useful constraints. To illustrate this, we write Eq. (16) as

$$(\eta_B^K)^{3/4} \eta_{e,NT}^K \simeq 3 \times 10^{-2} L_{37} \theta_{0.2}^{7/2} \beta_{0.5}^{7/4} P_{43}^{-7/4} r_5^{-3} \chi_{-1}^{-1}, \quad (18)$$

where $\chi_{-1} = \chi_{kev}^K / 10^{-1}$. Figure 1 also shows $\eta_B^K + \eta_{e,NT}^K$ under the above constraint. Because this sum should not significantly exceed one, we obtain $\chi_{kev}^K \gtrsim 0.01$. This places tight constraints on the spectrum. If we

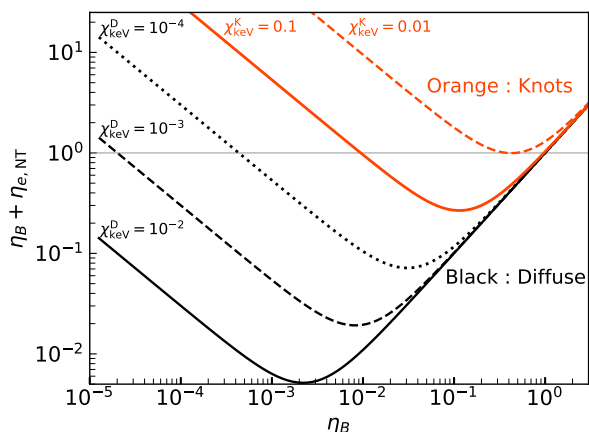


Figure 1. The sum of non-thermal electron and magnetic energy as a function of η_B , under the constraints from X-ray observation: Eq. (17) for the diffuse jet and Eq. (18) for the knots. This sum cannot (significantly) exceed one, which constrains these parameters.

use $p_{e,L} \simeq 2.3$ as an example, then $E_{e,kev}$ should be nearly equal to (or smaller than) $E_{e,br}$ to satisfy this constraint. If we instead use $p_{e,L} \simeq 2.06$ as derived for the diffuse jet, $E_{e,kev}$ still need be relatively close to the break: $E_{e,kev} \lesssim 10 E_{e,br}$. In the latter case, χ_{kev}^K can be as high as 0.1.

3.3. Conditions in the Jet

X-ray observations allow three distinct scenarios for the physical conditions in the diffuse jet.

- (i) Strongly magnetized, $\eta_B^D \sim 1$
- (ii) non-thermal electron dominant, $\eta_{e,NT}^D \sim 1$
- (iii) Thermal plasma dominant, $\eta_{Th}^D \sim 1$

Case (i): If the entire jet is strongly magnetized, the knot would also have a high magnetization, $\eta_B^K \sim 1$. The large difference in luminosity densities would be due to higher electron energy densities in the knots, implying efficient particle (re-)acceleration taking place there.

Case (ii): If the jet total energy is mostly carried by non-thermal electrons, the diffuse jet should be very weakly magnetized: $\eta_B^D \sim 4 \times 10^{-4} (\chi_{-4})^{-4/3}$ (Eq. 17). In this case, amplification of the magnetic field would be needed to explain the compact knots.

Case (iii): If the bulk of the jet energy is carried by thermal particles, the jet magnetization would be relatively weak because $\eta_B^D + \eta_{e,NT}^D \ll 1$. In the knot region, we would expect larger values of η_B^K and $\eta_{e,NT}^K$, but the thermal particles should still have most of the energy there. A plausible realization of such a scenario is equipartition between the magnetic field and the non-thermal electrons, $\eta_B^K \simeq \eta_{e,NT}^K$, which minimizes the energy requirement for these two components.

Next, we show that only case (iii) is allowed by the VHE data.

4. FURTHER CONSTRAINTS FROM VHE DATA

4.1. VHE Emission from the Jet

In this section, we assume that the observed VHE emission is produced by IC scattering in the Thomson regime, which is valid if the target photon is dominantly provided by far-IR radiation. The observed keV and VHE luminosity relates as $L_{kev}/L_{VHE} = w_B/w_{ph}$, where w_{ph} is the radiation energy density. Therefore, the following photon field energy densities would be required, depending on the production site of VHE emission:

$$w_{ph} = \frac{L_{VHE}}{L_{kev}^D} w_B^D \simeq w_B^D \text{ (diffuse jet),} \quad (19)$$

$$w_{ph} = \frac{L_{VHE}}{NL_{kev}^K} w_B^K \simeq 2w_B^K \text{ (knots),}$$

where $N (\simeq 30)$ is the number of knots.

Since knots have much higher synchrotron luminosity density than the diffuse jet, we would naturally expect $w_B^K \geq w_B^D$. Then, if VHE emission is dominated by knots, they should have locally enhanced photon fields. To be relevant, the knot additional photon field should have an energy density comparable to that of the magnetic field. The luminosity should be

$$L_{\text{ph}}^{\text{add}} = 4\pi r^2 c w_B^K, \quad (20)$$

$$\simeq 5 \times 10^{40} \eta_B^K r_5^2 P_{43} \theta_{0.2}^{-2} \beta_{0.5}^{-1} \text{ erg s}^{-1}.$$

Since the knot magnetic field is $\eta_B^K \gtrsim 10^{-2}$ from X-ray observation (Figure 1), a luminous photon source brighter than $5 \times 10^{38} \text{ erg s}^{-1}$ would be needed. This is much brighter than the X-ray luminosity of each knot, which indicates that synchrotron self-Compton cannot be sufficient. In principle, luminous stars could provide this photon field, but in that case, the production of VHE should proceed in the Klein-Nishina regime, significantly decreasing the efficiency of the IC process. Therefore, we regard this possibility as unlikely and consider the diffuse jet as the origin of the VHE emission.

If the target photons are generated inside the jet, the required photon luminosity is

$$\pi R Z c w_{\text{ph}} = 3 \times 10^{44} \eta_B^D \frac{P_{43} Z_3}{\theta_{0.2}^2} \text{ erg s}^{-1}. \quad (21)$$

This scenario necessitates a relatively small jet magnetization, $\eta_B^D \lesssim 0.03$, because otherwise the required luminosity would exceed the total jet power. The required luminosity can be decreased by a factor of $R/Z \sim 0.2$, if we assume that the target photons are strongly beamed along the jet axis (e.g., if emitted by the highly relativistic inner jet, see Bednarek 2019), but this still requires η_B^D well below 0.1.

If the soft photons are supplied from external sources, their luminosity should be

$$w_{\text{ph}} 4\pi d^2 c = 2 \times 10^{45} \eta_B^D \frac{P_{43} d_1^2}{\theta_{0.2}^2 \beta_{0.5}} \text{ erg s}^{-1} \quad (22)$$

where $d = 1d_1 \text{ kpc}$ is the distance from the emitting region to the source of soft photons. This scenario necessitates a relatively small jet magnetization, $\eta_B^D \lesssim 0.03$, because otherwise the luminosity of the host galaxy would not be sufficient.

Both internal and external sources of target photons require $\eta_B^D < 0.03$. This excludes the possibility of a strongly magnetized jet (case i). Figure 2 shows the jet magnetization parameter in the diffuse jet as a function of the photon energy density. If we adopt luminosities of the host galaxy as the target photon (Table 1), the

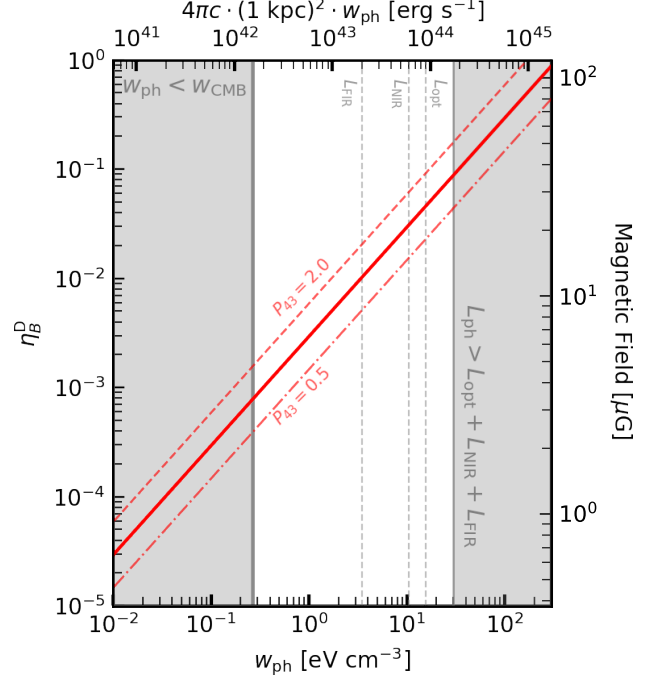


Figure 2. Jet magnetization that is required for explaining VHE emission, as a function of soft photon energy density. The solid line adopts $P_{43} = 1$, while other two lines show the cases when P_{43} is changed to 2 (dashed) and 0.5 (dot-dashed). Other model parameters are fixed to the value as adopted in the main text.

jet magnetization would be $\eta_B^D \sim 10^{-2}$. It also shows that the jet magnetization should satisfy $\eta_B^D \gtrsim 10^{-3}$, because otherwise the emission produced on the cosmic microwave background radiation would be brighter than observed. This excludes the case of a very weakly magnetized jet (case ii). We conclude that the thermal plasma dominates the jet energetics (case iii).

Thus far, we have shown that thermal particles carry most of the energy in the diffuse jet. It may not seem straightforward to relate this with the energetics in knots, because they locally have very different conditions. However, considering that knots are likely produced by the same material that composes the diffuse jet, in which non-thermal electrons and magnetic field make only $\simeq 5\%$ of the energy, thermal plasma is likely dominant also in the knot regions. In principle, we cannot rule out a possibility that magnetic fields are amplified to $\eta_B^K \simeq \eta_{\text{Th}}^K$, but it would require very efficient conversion of thermal energy to the magnetic field. A more feasible scenario is to keep most of the energy in thermal particles in the knot region by minimizing $\eta_B^K + \eta_{e,\text{NT}}^K$ (i.e., equipartition), with η_B^K and $\eta_{e,\text{NT}}^K$ amplified by a factor of $\mathcal{O}(1)$ compared to the diffuse jet. This argument favors $\eta_B^K \simeq \eta_{e,\text{NT}}^K \sim 0.1$ (see Fig. 1). This results in a relatively

weak magnetic field, $B^K \sim 40 \mu\text{G}$, consistent with the observed upper limits for two bright knots ($B^K < 80 \mu\text{G}$; Snios et al. 2019).

4.2. Implications for Particle Acceleration

The dominance of thermal particles implies a relatively small magnetic field even in the knot region. Therefore, particles produced in knots can travel a distance of

$$\begin{aligned} r_{\text{syn}} &= c\beta t_{\text{syn}}^{\text{K}}, \\ &\simeq 60 \left(\frac{\hbar\omega}{1 \text{ keV}} \right)^{-1/2} \left(\frac{\eta_{\text{B}}^{\text{K}}}{0.1} \right)^{-3/4} P_{43}^{-3/4} \theta_{0.2}^{3/2} \beta_{0.5}^{7/4} \text{ pc}. \end{aligned} \quad (23)$$

before losing energy to the synchrotron cooling. This is significantly larger than typical knot size, which indicates that they escape from the knots and contribute to the diffuse emission. The electron power supplied by escaping particles from each knot is $L_{\text{kev}}^{\text{K}} t_{\text{syn}}^{\text{K}} / t_{\text{adv}}^{\text{K}}$, where $t_{\text{adv}}^{\text{K}} = r / \beta c$ is the advection time in the knot. They would cool down in the diffuse jet, radiating with an X-ray luminosity of

$$\begin{aligned} L_{\text{kev}} &\sim \frac{\xi}{2} N L_{\text{kev}}^{\text{K}} \frac{t_{\text{syn}}^{\text{K}}}{t_{\text{adv}}^{\text{K}}} \\ &\sim 90 L_{\text{kev}}^{\text{K}} \left(\frac{\xi}{0.5} \right) \left(\frac{N}{30} \right) P_{43}^{-3/4} r_5^{-1} \beta_{0.5}^{7/4} \theta_{0.2}^{3/2} \\ &\sim 9 \times 10^{38} \text{ erg s}^{-1}, \end{aligned} \quad (24)$$

where $1/2$ roughly accounts for the synchrotron and IC cooling. The parameter ξ takes the difference in magnetic fields between diffuse jet and knots: since $E_{e,\text{kev}} \propto (\eta_{\text{B}})^{-1/4}$, the energy in keV-emitting electrons differ by a factor of $\xi \sim (\eta_{\text{B}}^{\text{K}} / \eta_{\text{B}}^{\text{D}})^{(2-\rho_{\text{H}})/4} \sim 0.5$. This estimate is remarkably close to the diffuse luminosity, suggesting that the particles accelerated in the compact knots may play an essential role in producing the jet diffuse emission.

5. HADRONIC SCENARIO

Here, we assess the contribution of hadronic processes to the observed VHE emission. We assume that a sub-volume \mathcal{V} of the jet produces gamma rays via pp interactions. The total energy in non-thermal protons in this region is

$$\begin{aligned} W_{p,\text{NT}} &= w_{\text{jet}} \eta_{p,\text{NT}} \mathcal{V}, \\ &\simeq 6 \times 10^{54} \eta_{p,\text{NT}} P_{43} Z_3 \beta_{0.5}^{-1} f_{\text{V}} \text{ erg}, \end{aligned} \quad (25)$$

where $f_{\text{V}} = \mathcal{V} / V_{\text{jet}}$ is the filling factor of the production sites. These protons produce VHE gamma-rays on a

timescale of $t_{pp} = 10^{15} n^{-1}$ s, where n is the gas density in the cgs unit. The luminosity is then

$$\begin{aligned} L_{\text{VHE},pp} &\sim \kappa \frac{\chi_{\text{TeV}} W_{p,\text{NT}}}{t_{pp}}, \\ &\sim 10^{39} \eta_{p,\text{NT}} n f_{\text{V}} P_{43} Z_3 \beta_{0.5}^{-1} \text{ erg s}^{-1}, \end{aligned} \quad (26)$$

where $\chi_{\text{TeV}} W_{p,\text{NT}}$ is the energy of non-thermal protons in the TeV regime and $\kappa \sim 0.17$ is the fraction of the proton energy converted into gamma-rays. To explain the observed luminosity, $7 \times 10^{38} \text{ erg s}^{-1}$, the target density should be very high:

$$n f_{\text{V}} \sim 70 \left(\frac{\eta_{p,\text{NT}}}{0.1} \right)^{-1} \left(\frac{\chi_{\text{TeV}}}{0.1} \right)^{-1} P_{43}^{-1} Z_3^{-1} \beta_{0.5} \text{ cm}^{-3}. \quad (27)$$

If the target gas were involved with the jet motion, the kinetic energy flux would significantly exceed the total jet energy flux (Eq. 2):

$$\begin{aligned} F_{\text{gas}} &= (\Gamma_{\text{jet}} - 1) m_{\text{p}} c^2 n f_{\text{V}} \beta c \\ &\simeq 3 \times 10^6 f_{\text{V}} n \text{ erg s}^{-1} \text{ cm}^{-2}, \end{aligned} \quad (28)$$

Therefore, it is difficult to explain the observed VHE emission by hadronic emission alone. However, some contributions may be possible from the gamma-ray production on dense external cloud or stellar winds (Barkov et al. 2010, 2012).

6. CONCLUSION

In this work, we study the origin of non-thermal emission and physical conditions in the kpc-jet of Cen A. By combining X-ray and VHE data, we determine the jet magnetization to be $\eta_{\text{B}}^{\text{D}} \sim 10^{-2}$ in the kpc-jet. This result is consistent with a recent study on FR II radio galaxies (Sikora et al. 2020). In knot regions, the energy densities in the magnetic field and non-thermal electrons should be amplified to an equipartition value, $\eta_{\text{B}}^{\text{K}} \simeq \eta_{e,\text{NT}}^{\text{K}} \sim 0.1$. Such a weak magnetic field implies that most particles leave knots uncooled. We find that it remains viable that entire jet X-ray and VHE emission is produced by particles that are accelerated at and escaped from knots. More detailed modeling is needed to test this scenario.

ACKNOWLEDGEMENTS

We thank Felix Aharonian, Maxim Barkov, Valentí Bosch-Ramon, Jun Kataoka, Frank Rieger, and Marek Sikora for useful comments. This research made use of the NASA/IPAC Extragalactic Database (NED), which is operated by the Jet Propulsion Laboratory, California Institute of Technology, under contract with the National Aeronautics and Space Administration. T.S. is supported by Research Fellowship of Japan

Society for the Promotion of Science (JSPS), and also supported by JSPS KAKENHI Grant Number JP18J20943. Y.I. is supported by JSPS KAKENHI Grant Number JP16K13813, JP18H05458, JP19K14772, pro-

gram of Leading Initiative for Excellent Young Researchers, MEXT, Japan, and RIKEN iTHEMS Program. D.K. is supported by JSPS KAKENHI Grant Numbers JP18H03722, JP24105007, and JP16H02170.

REFERENCES

- Abdalla, H., Adam, R., Aharonian, F., et al. 2020, *Nature*, 582, 356, doi: [10.1038/s41586-020-2354-1](https://doi.org/10.1038/s41586-020-2354-1)
- Ackermann, M., Anantua, R., Asano, K., et al. 2016, *ApJL*, 824, L20, doi: [10.3847/2041-8205/824/2/L20](https://doi.org/10.3847/2041-8205/824/2/L20)
- Barkov, M. V., Aharonian, F. A., & Bosch-Ramon, V. 2010, *ApJ*, 724, 1517, doi: [10.1088/0004-637X/724/2/1517](https://doi.org/10.1088/0004-637X/724/2/1517)
- Barkov, M. V., Bosch-Ramon, V., & Aharonian, F. A. 2012, *ApJ*, 755, 170, doi: [10.1088/0004-637X/755/2/170](https://doi.org/10.1088/0004-637X/755/2/170)
- Beckmann, V., Jean, P., Lubiński, P., Soldi, S., & Terrier, R. 2011, *A&A*, 531, A70, doi: [10.1051/0004-6361/201016020](https://doi.org/10.1051/0004-6361/201016020)
- Bednarek, W. 2019, *MNRAS*, 483, 1003, doi: [10.1093/mnras/sty3027](https://doi.org/10.1093/mnras/sty3027)
- Bednarek, W., & Banasiński, P. 2015, *ApJ*, 807, 168, doi: [10.1088/0004-637X/807/2/168](https://doi.org/10.1088/0004-637X/807/2/168)
- Blandford, R. D., & Koenigl, A. 1979, *Astrophys. Lett.*, 20, 15
- Blandford, R. D., & Payne, D. G. 1982, *MNRAS*, 199, 883, doi: [10.1093/mnras/199.4.883](https://doi.org/10.1093/mnras/199.4.883)
- Blandford, R. D., & Znajek, R. L. 1977, *MNRAS*, 179, 433, doi: [10.1093/mnras/179.3.433](https://doi.org/10.1093/mnras/179.3.433)
- Cappellari, M., Neumayer, N., Reunanen, J., et al. 2009, *MNRAS*, 394, 660, doi: [10.1111/j.1365-2966.2008.14377.x](https://doi.org/10.1111/j.1365-2966.2008.14377.x)
- Celotti, A., & Ghisellini, G. 2008, *MNRAS*, 385, 283, doi: [10.1111/j.1365-2966.2007.12758.x](https://doi.org/10.1111/j.1365-2966.2007.12758.x)
- Chiaberge, M., Capetti, A., & Celotti, A. 2001, *MNRAS*, 324, L33, doi: [10.1046/j.1365-8711.2001.04642.x](https://doi.org/10.1046/j.1365-8711.2001.04642.x)
- Ghisellini, G., Tavecchio, F., Foschini, L., et al. 2010, *MNRAS*, 402, 497, doi: [10.1111/j.1365-2966.2009.15898.x](https://doi.org/10.1111/j.1365-2966.2009.15898.x)
- Goodger, J. L., Hardcastle, M. J., Croston, J. H., et al. 2010, *ApJ*, 708, 675, doi: [10.1088/0004-637X/708/1/675](https://doi.org/10.1088/0004-637X/708/1/675)
- H. E. S. S. Collaboration, Abdalla, H., Abramowski, A., et al. 2018, *A&A*, 619, A71, doi: [10.1051/0004-6361/201832640](https://doi.org/10.1051/0004-6361/201832640)
- Hardcastle, M. J., & Croston, J. H. 2011, *MNRAS*, 415, 133, doi: [10.1111/j.1365-2966.2011.18678.x](https://doi.org/10.1111/j.1365-2966.2011.18678.x)
- Hardcastle, M. J., Kraft, R. P., & Worrall, D. M. 2006, *MNRAS*, 368, L15, doi: [10.1111/j.1745-3933.2006.00146.x](https://doi.org/10.1111/j.1745-3933.2006.00146.x)
- Hardcastle, M. J., Worrall, D. M., Kraft, R. P., et al. 2003a, *ApJ*, 593, 169, doi: [10.1086/376519](https://doi.org/10.1086/376519)
- . 2003b, *ApJ*, 593, 169, doi: [10.1086/376519](https://doi.org/10.1086/376519)
- Harris, G. L. H., Rejkuba, M., & Harris, W. E. 2010, *PASA*, 27, 457, doi: [10.1071/AS09061](https://doi.org/10.1071/AS09061)
- Horiuchi, S., Meier, D. L., Preston, R. A., & Tingay, S. J. 2006, *PASJ*, 58, 211, doi: [10.1093/pasj/58.2.211](https://doi.org/10.1093/pasj/58.2.211)
- Inoue, Y., & Tanaka, Y. T. 2016, *ApJ*, 828, 13, doi: [10.3847/0004-637X/828/1/13](https://doi.org/10.3847/0004-637X/828/1/13)
- Kataoka, J., Stawarz, L., Aharonian, F., et al. 2006, *ApJ*, 641, 158, doi: [10.1086/500407](https://doi.org/10.1086/500407)
- Komissarov, S. S., Barkov, M. V., Vlahakis, N., & Königl, A. 2007, *MNRAS*, 380, 51, doi: [10.1111/j.1365-2966.2007.12050.x](https://doi.org/10.1111/j.1365-2966.2007.12050.x)
- Kraft, R. P., Forman, W. R., Jones, C., et al. 2002, *ApJ*, 569, 54, doi: [10.1086/339062](https://doi.org/10.1086/339062)
- Mao, J., & Wang, J. 2007, *ApJL*, 669, L13, doi: [10.1086/523270](https://doi.org/10.1086/523270)
- McKinney, J. C., Tchekhovskoy, A., & Blandford, R. D. 2012, *MNRAS*, 423, 3083, doi: [10.1111/j.1365-2966.2012.21074.x](https://doi.org/10.1111/j.1365-2966.2012.21074.x)
- Sanders, R. H. 1983, *ApJ*, 266, 73, doi: [10.1086/160760](https://doi.org/10.1086/160760)
- Sikora, M., Nalewajko, K., & Madejski, G. M. 2020, arXiv e-prints, arXiv:2004.03606, <https://arxiv.org/abs/2004.03606>
- Sironi, L., Petropoulou, M., & Giannios, D. 2015, *MNRAS*, 450, 183, doi: [10.1093/mnras/stv641](https://doi.org/10.1093/mnras/stv641)
- Snios, B., Wykes, S., Nulsen, P. E. J., et al. 2019, *ApJ*, 871, 248, doi: [10.3847/1538-4357/aafaf3](https://doi.org/10.3847/1538-4357/aafaf3)
- Tanada, K., Kataoka, J., & Inoue, Y. 2019, *ApJ*, 878, 139, doi: [10.3847/1538-4357/ab2233](https://doi.org/10.3847/1538-4357/ab2233)
- Tavecchio, F., Maraschi, L., & Ghisellini, G. 1998, *ApJ*, 509, 608, doi: [10.1086/306526](https://doi.org/10.1086/306526)
- Tingay, S. J., & Lenc, E. 2009, *AJ*, 138, 808, doi: [10.1088/0004-6256/138/3/808](https://doi.org/10.1088/0004-6256/138/3/808)
- Torres-Albà, N., & Bosch-Ramon, V. 2019, *A&A*, 623, A91, doi: [10.1051/0004-6361/201833697](https://doi.org/10.1051/0004-6361/201833697)
- Vieyro, F. L., Torres-Albà, N., & Bosch-Ramon, V. 2017, *A&A*, 604, A57, doi: [10.1051/0004-6361/201630333](https://doi.org/10.1051/0004-6361/201630333)
- Wykes, S., Croston, J. H., Hardcastle, M. J., et al. 2013, *A&A*, 558, A19, doi: [10.1051/0004-6361/201321622](https://doi.org/10.1051/0004-6361/201321622)
- Wykes, S., Snios, B. T., Nulsen, P. E. J., et al. 2019, *MNRAS*, 485, 872, doi: [10.1093/mnras/stz348](https://doi.org/10.1093/mnras/stz348)
- Zhang, J., Liang, E.-W., Zhang, S.-N., & Bai, J. M. 2012, *ApJ*, 752, 157, doi: [10.1088/0004-637X/752/2/157](https://doi.org/10.1088/0004-637X/752/2/157)